

**HOMOLOGY MODELING AND STRUCTURAL STUDIES OF POTENTIALLY  
SECRETED CELL WALL PROTEIN ZN-CU SOD FROM *NEUROSPORA CRASSA***

S. K. Gousia, T. V. Padmavathi, N. V. Ramana and J. Naveena Lavanya Latha\*

Department of Biotechnology, Krishna University, Machilipatnam-521001.

\*Corresponding Author: Dr. J. Naveena Lavanya Latha

Department of Biotechnology, Krishna University, Machilipatnam-521001.

Article Received on 01/08/2017

Article Revised on 22/08/2017

Article Accepted on 13/09/2017

**ABSTRACT**

**Background:** The cell wall may work as an obstacle by keeping proteins from spilling into the medium and go about as a system for revealing cell wall proteins (CWPs) to the cell surface. Metal particles, for example, copper, iron, and zinc and others assume a crucial part in living life forms fundamentally by virtue of their relationship with proteins, which are referred to as metalloproteins. Copper essentiality holds both its action in structural stabilization and its redox capacity, which is utilized by metalloenzymes that catalyze electron exchange responses. The most advanced utilitarian classifications in the Zn proteome were those identified with transcription, cell cycle, and DNA processing, and in addition protein in fate and modification. **Methods:** The stereo chemical quality of the protein model was checked by using insilico analysis with PROCHECK and QMEAN servers. The metal binding sites were determined by CHED. **Results:** In the present study, the authors found that the protein under study contained 7 metal binding sites shows highest metal binding probability for the metal namely calcium in sites 2, 3, 4 & 7 with the metal probability of **0.691595, 0.627722, 0.398702 & 0.304824; Copper** in sites 1&5 with the probability of **0.407987 & 0.520100** and zinc in sites 1, 4, 6 & 7 with the probability of **0.473539, 0.411537, 0.595477 & 0.527491** were showed. **Conclusions:** The result of the study may be a guiding point for further investigations on Zn-Cu SOD protein and metal binding sites. **Significant Statement:** The Zn-Cu SOD protein extracted from cells of *N.crassa* was found to possess 7 metal binding sites of which four were found to have high probability towards calcium, two for copper and four sites for zinc.

**KEYWORDS:** Zn-Cu SOD, Cell binding protein, *Neurospora crassa*, homology modeling, metal binding sites.

**INTRODUCTION**

The fungal cell wall is a crucial organelle that empowers cells to oppose inward turgor weights which, in appressoria of plant pathogens, may achieve values up to 8 MPa. The cell wall is likewise of key significance for keeping up cell morphology, take-up of substances, communications with plasma film proteins, flagging, and assurance against unfriendly conditions in the cell environment<sup>[1]</sup>. The substantial assorted qualities of involved organic parts of CWPs incorporate cell wall biosynthesis and attachment. For pathogenic microorganisms, for example, organisms and oomycetes, CWPs likewise can give assurance against host protection responses. Bond to host tissues is a vital property in pathogenesis and, as a rule, key for destructiveness<sup>[2]</sup>. Superoxide dismutase (SOD) proteins catalyze the breakdown of superoxide into hydrogen peroxide and water. They are focal controllers of receptive oxygen species (ROS) levels. Cu, Zn SOD is one of the real proteins required in the cell reaction to hoisted levels of zinc particles and its defensive impacts against zinc poisonous quality may include both its metal-restricting limit and its enzymatic action<sup>[3]</sup>. Fungal cells must procure zinc for legitimate advancement in

their life cycle, not withstanding when they are saprophytes or amid the contamination procedure. Some zinc-restricting proteins are additionally required in contagious harmfulness. Superoxide dismutase's (Sods) are the focal compounds in parasites connected with the detoxification of ROS produced by host cells amid host-pathogen associations. Example of a zinc-binding protein that is communicated to decrease the bioavailability of zinc is calprotectin, an individual from the S100 group of metal-restricting proteins. Calprotectin was found to diminish the development of differing fungal species in vitro. Cu can turn out to be high in enacted macrophages, and reliable with this, *C. albicans* mutants blemished in Cu detoxification demonstrate impedances in macrophage attack. Cu can likewise turn out to be high in particular host specialties, for example, in lungs contaminated with *C. neoformans* and in the circulation system amid *C. albicans* and *C. neoformans* intrusion<sup>[4]</sup>. The *A. fumigatus* genome contains four qualities encoding Sods, two of which are explained as copper/zinc-subordinate (Sod1 and Sod4). *A. fumigatus* cells without the SOD1 quality are extremely touchy to menadione, a ROS producing operator, however the

harmfulness of cells without this quality is not influenced.

## METHODS

**2D gel analysis of cell wall proteins:** The two-dimensional natural action remains a technique of selection for the alternate approaches that are used for the proteomic analysis of membrane proteins.

**BLAST P, multiple sequence alignment and phylogenetic tree construction:** The amino acid sequence obtained by MALDI-TOF/MS analysis of protein Zn-Cu SOD isolated from cell walls of *Neurospora crassa*. According Altschul et al., 1997<sup>[5]</sup>, the protein sequences are scanned by using the BLAST P algorithm one can obtain the homologous protein sequences from the available protein sequences of various organisms. The target sequence was searched with BLAST against the primary amino acid sequence contained in the SMTL<sup>[6]</sup>. The obtained profile has then been searched against all profiles of the SMTL. Overall 184 templates were found (Table 1a). Models are built based on the target-template alignment using ProMod3. Coordinates which are conserved between the target and the template are copied from the template to the model. Insertions and deletions are remodeled using a fragment library. Side chains are then rebuilt. Finally, the geometry of the resulting model is regularized by using a force field. In case loop modelling with ProMod3 fails, an alternative model is built with PROMOD-II<sup>7</sup> or MODELLER<sup>[8]</sup>. Phylogenetic tree was then constructed using phylogeny.fr (<http://www.phylogeny.fr/>) to determine the evolutionary relationships<sup>[9-10]</sup>.

**Secondary structure prediction:** Secondary structure of Zn-Cu SOD family protein was predicted using SOPMA ([https://npsa-prabi.ibcp.fr/cgi-bin/npsa\\_automat.pl?page=npsa\\_sopma.html](https://npsa-prabi.ibcp.fr/cgi-bin/npsa_automat.pl?page=npsa_sopma.html)) tool in ExPASy.

**Homology modeling:** The sequence of Zn-Cu SOD was downloaded from the universal protein resource<sup>[11]</sup> (Uniprot KB) (<http://www.uniprot.org/>) (entry ID: G4U5N5). The suitable template for homology modeling was identified through searching Zn-Cu SOD on PDB using the BLAST P algorithm<sup>[12]</sup>. The 3D structure of Zn-Cu SOD was downloaded from PDB (Template PDB ID: 4n3t.1.A) as the template structure.

## Model validation

The quality of the homology model turned into confirmed by means of assessing the stereo chemical quality of the model by using Ramachandran plot received from the RAMPAGE (<http://mordred.bioc.cam.ac.uk/~rapper/rampage.php>) server<sup>[13]</sup>. Affirm 3D<sup>[14]</sup> and ERRAT<sup>[15]</sup> were used to assess the amino acid environment from the UCLA-DOE server (<http://www.doe-mbi.ucla.edu/services>).

## Model Quality Estimation

The global and per-residue model quality has been assessed by the use of the QMEAN scoring function<sup>[16]</sup>. For advanced performance, weights of the individual QMEAN terms were trained mainly for SWISS-MODEL.

## Metal binding sites

Maximum of the metalloproteins, the buildups required in metallic limiting technique collectively within the tertiary shape to form the coupling site, yet are scattered alongside the amino corrosive association. In this paper the protein suggests perfect steel binding likelihood for metallic specifically for calcium, magnesium and zinc (Table 3).

## RESULTS AND DISCUSSION

The isolated cell wall fractions when subjected to 2D gel analysis resulted in ~24 proteins (Fig.1). MALDI TOF-MS analysis followed by mascot search with the obtained sequence revealed that the sequence of the Zn-Cu SOD sequence in UNIPORT KB revealed that the sequence is a Zn-Cu SOD protein from *Sordaria macrospora* (Fig.2).

## 2D gel analysis of cell wall proteins.

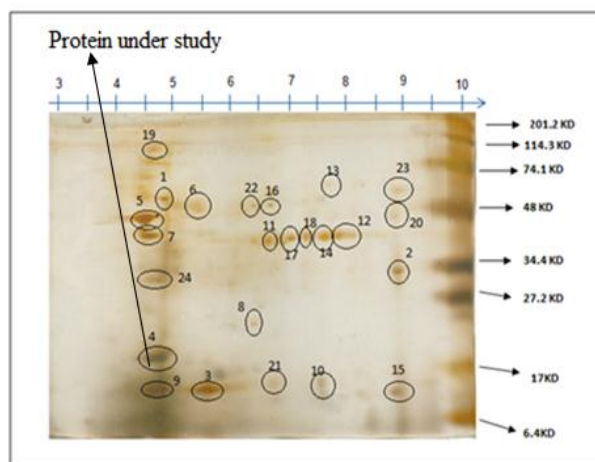


**Fig. 1: 2D gel analysis showing protein under study.**

Scanning of protein sequence databases using BLAST P obtained from MALDI-TOF/MS analysis of the purified lipase revealed that the protein is a hypothetical protein from Zn-Cu SOD with an entry ID: G4U5N5 shown in (Fig.2). Phylogram was constructed based on multiple sequence alignment using phylogeny.fr revealed that the Zn-Cu SOD was closely related to a conserved hypothetical protein from *Sordaria macrospora* was shown in (Fig.2).



Table. 1a.

Template	Seq Identity	Oligo-state	Found by	Method	Resolution	Seq Similarity	Coverage	Description
4n3t.1.A	38.00	monomer	HHblits	X-ray	1.40Å	0.39	0.60	Potential secreted Cu/Zn superoxide dismutase
5kbb.1.A	38.00	monomer	HHblits	X-ray	1.41Å	0.39	0.60	Cell surface Cu-only superoxide dismutase 5
5kbl.1.A	38.26	monomer	HHblits	X-ray	1.41Å	0.39	0.60	Cell surface Cu-only superoxide dismutase 5
5kbn.1.A	36.91	monomer	HHblits	X-ray	1.42Å	0.38	0.60	Cell surface Cu-only superoxide dismutase 5
5kbl.1.A	46.40	monomer	BLAST	X-ray	1.41Å	0.43	0.50	Cell surface Cu-only superoxide dismutase 5
4n3t.1.A	45.60	monomer	BLAST	X-ray	1.40Å	0.43	0.50	Potential secreted Cu/Zn superoxide dismutase
5kbb.1.A	45.60	monomer	BLAST	X-ray	1.41Å	0.43	0.50	Cell surface Cu-only superoxide dismutase 5
5kbn.1.A	44.80	monomer	BLAST	X-ray	1.42Å	0.42	0.50	Cell surface Cu-only superoxide dismutase 5
1to4.1.A	30.60	homo-dimer	HHblits	X-ray	1.55Å	0.35	0.54	Superoxide dismutase
3ce1.1.A	26.47	homo-dimer	HHblits	X-ray	1.20Å	0.33	0.55	Superoxide dismutase [Cu-Zn]
1srd.1.A	32.58	homo-tetramer	HHblits	X-ray	2.00Å	0.36	0.53	COPPER,ZINC SUPEROXIDE DISMUTASE
3gtt.1.A	28.57	homo-dimer	HHblits	X-ray	2.40Å	0.35	0.54	Superoxide dismutase [Cu-Zn]
4bcy.1.A	30.83	monomer	HHblits	X-ray	1.27Å	0.35	0.54	SUPEROXIDE DISMUTASE [CU-ZN]
3s0p.1.A	31.82	homo-dimer	HHblits	X-ray	3.00Å	0.35	0.53	Superoxide dismutase [Cu-Zn], chloroplastic
3hog.1.A	31.82	homo-dimer	HHblits	X-ray	1.85Å	0.35	0.53	Superoxide dismutase [Cu-Zn], chloroplastic
3km2.2.B	31.82	homo-dimer	HHblits	X-ray	3.10Å	0.35	0.53	Superoxide dismutase [Cu-Zn], chloroplastic
2xjk.1.A	30.08	monomer	HHblits	X-ray	1.45Å	0.34	0.54	SUPEROXIDE DISMUTASE [CU-ZN]
3ltv.1.A	27.82	homo-dimer	HHblits	X-ray	2.45Å	0.34	0.54	Superoxide dismutase [Cu-Zn]
1mfm.1.A	29.32	monomer	HHblits	X-ray	1.02Å	0.34	0.54	PROTEIN (COPPER,ZINC SUPEROXIDE DISMUTASE)
1ba9.1.A	29.32	monomer	HHblits	NMR	NA	0.34	0.54	SUPEROXIDE DISMUTASE
1kmg.1.A	29.32	monomer	HHblits	NMR	NA	0.34	0.54	Superoxide Dismutase
1rk7.1.A	29.32	monomer	HHblits	NMR	NA	0.34	0.54	Superoxide dismutase [Cu-Zn]
3gtv.1.A	29.32	homo-dimer	HHblits	X-ray	2.20Å	0.34	0.54	Superoxide dismutase [Cu-Zn]
2gbt.1.A	30.08	homo-dimer	HHblits	X-ray	1.70Å	0.34	0.54	Superoxide dismutase [Cu-Zn]
2gbt.2.A	30.08	homo-dimer	HHblits	X-ray	1.70Å	0.34	0.54	Superoxide dismutase [Cu-Zn]
1dsw.1.A	28.57	monomer	HHblits	NMR	NA	0.34	0.54	SUPEROXIDE DISMUTASE (CU-ZN)
1flg.1.A	24.63	homo-dimer	HHblits	X-ray	1.35Å	0.33	0.54	COPPER-ZINC SUPEROXIDE DISMUTASE
1n18.1.A	29.32	homo-dimer	HHblits	X-ray	2.00Å	0.34	0.54	Superoxide dismutase [Cu-Zn]
1fun.1.A	29.32	homo-dimer	HHblits	X-ray	2.85Å	0.34	0.54	SUPEROXIDE DISMUTASE
2af2.1.A	29.32	homo-dimer	HHblits	NMR	NA	0.34	0.54	Superoxide dismutase [Cu-Zn]
2af2.1.B	29.32	homo-dimer	HHblits	NMR	NA	0.34	0.54	Superoxide dismutase [Cu-Zn]
113n.1.A	29.32	homo-dimer	HHblits	NMR	NA	0.34	0.54	superoxide dismutase [Cu-Zn]
113n.1.B	29.32	homo-dimer	HHblits	NMR	NA	0.34	0.54	superoxide dismutase [Cu-Zn]
2lu5.1.A	29.32	monomer	HHblits	NMR	NA	0.34	0.54	Superoxide dismutase [Cu-Zn]
1sos.1.A	29.32	homo-dimer	HHblits	X-ray	2.50Å	0.34	0.54	SUPEROXIDE DISMUTASE
1ptz.1.A	29.32	homo-dimer	HHblits	X-ray	1.80Å	0.34	0.54	Superoxide dismutase [Cu-Zn]
1ptz.1.B	29.32	homo-dimer	HHblits	X-ray	1.80Å	0.34	0.54	Superoxide dismutase [Cu-Zn]
4oh2.1.A	29.32	homo-dimer	HHblits	X-ray	2.38Å	0.34	0.54	Superoxide dismutase [Cu-Zn]

4oh2.2.A	29.32	homo-dimer	HHblits	X-ray	2.38Å	0.34	0.54	Superoxide dismutase [Cu-Zn]
4oh2.2.B	29.32	homo-dimer	HHblits	X-ray	2.38Å	0.34	0.54	Superoxide dismutase [Cu-Zn]
4oh2.3.A	29.32	homo-dimer	HHblits	X-ray	2.38Å	0.34	0.54	Superoxide dismutase [Cu-Zn]
4oh2.4.A	29.32	homo-dimer	HHblits	X-ray	2.38Å	0.34	0.54	Superoxide dismutase [Cu-Zn]
4oh2.5.A	29.32	homo-dimer	HHblits	X-ray	2.38Å	0.34	0.54	Superoxide dismutase [Cu-Zn]
3ecw.1.A	28.57	homo-dimer	HHblits	X-ray	2.15Å	0.34	0.54	Superoxide dismutase [Cu-Zn]
1n19.1.A	28.57	homo-dimer	HHblits	X-ray	1.86Å	0.34	0.54	Superoxide Dismutase [Cu-Zn]
3qqd.1.A	28.57	homo-dimer	HHblits	X-ray	1.65Å	0.34	0.54	Superoxide dismutase [Cu-Zn]
3qqd.1.B	28.57	homo-dimer	HHblits	X-ray	1.65Å	0.34	0.54	Superoxide dismutase [Cu-Zn]
2zky.1.A	28.57	homo-dimer	HHblits	X-ray	2.40Å	0.34	0.54	Superoxide dismutase [Cu-Zn]
1ozu.1.A	28.57	homo-dimer	HHblits	X-ray	1.30Å	0.34	0.54	Superoxide dismutase [Cu-Zn]
1ozu.1.B	28.57	homo-dimer	HHblits	X-ray	1.30Å	0.34	0.54	Superoxide dismutase [Cu-Zn]
3h2p.1.A	28.57	homo-dimer	HHblits	X-ray	1.55Å	0.34	0.54	Superoxide dismutase [Cu-Zn]
3h2p.1.B	28.57	homo-dimer	HHblits	X-ray	1.55Å	0.34	0.54	Superoxide dismutase [Cu-Zn]
1hl4.1.A	28.57	homo-dimer	HHblits	X-ray	1.82Å	0.34	0.54	SUPEROXIDE DISMUTASE
1spd.1.B	28.57	homo-dimer	HHblits	X-ray	2.40Å	0.34	0.54	SUPEROXIDE DISMUTASE
1spd.1.A	28.57	homo-dimer	HHblits	X-ray	2.40Å	0.34	0.54	SUPEROXIDE DISMUTASE
1p1v.1.A	28.57	homo-dimer	HHblits	X-ray	1.40Å	0.34	0.54	Superoxide dismutase [Cu-Zn]
4b3e.1.A	28.57	homo-dimer	HHblits	X-ray	2.15Å	0.34	0.54	SUPEROXIDE DISMUTASE [CU-ZN]
2q2l.1.A	30.53	homo-dimer	HHblits	X-ray	2.37Å	0.35	0.53	Superoxide Dismutase
2r27.1.A	28.57	homo-dimer	HHblits	X-ray	2.00Å	0.34	0.54	Superoxide dismutase [Cu-Zn]
2wyz.1.A	27.82	homo-dimer	HHblits	X-ray	1.70Å	0.34	0.54	SUPEROXIDE DISMUTASE [CU-ZN]
2wyt.1.B	27.82	homo-dimer	HHblits	X-ray	1.00Å	0.34	0.54	SUPEROXIDE DISMUTASE [CU-ZN]
3ecv.1.A	28.57	homo-dimer	HHblits	X-ray	1.90Å	0.34	0.54	Superoxide dismutase [Cu-Zn]
1uxl.4.B	28.57	homo-dimer	HHblits	X-ray	1.60Å	0.34	0.54	SUPEROXIDE DISMUTASE [CU-ZN]
4a7u.1.A	28.57	homo-dimer	HHblits	X-ray	0.98Å	0.34	0.54	SUPEROXIDE DISMUTASE [CU-ZN]
1fla.1.A	23.88	homo-dimer	HHblits	X-ray	1.80Å	0.33	0.54	COPPER-ZINC SUPEROXIDE DISMUTASE
1f18.1.A	23.88	homo-dimer	HHblits	X-ray	1.70Å	0.33	0.54	COPPER-ZINC SUPEROXIDE DISMUTASE
4a7g.1.A	28.57	hetero-oligomer	HHblits	X-ray	1.24Å	0.34	0.54	SUPEROXIDE DISMUTASE [CU-ZN]
1uxm.1.A	27.82	homo-dimer	HHblits	X-ray	1.90Å	0.34	0.54	SUPEROXIDE DISMUTASE [CU-ZN]
3gzq.1.A	27.82	homo-dimer	HHblits	X-ray	1.40Å	0.34	0.54	Superoxide dismutase [Cu-Zn]

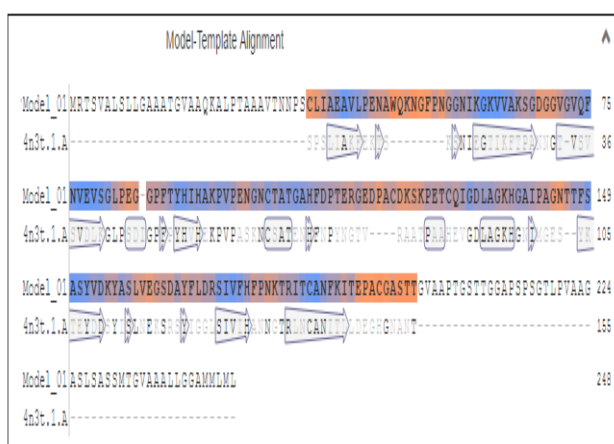


Fig. 5a.

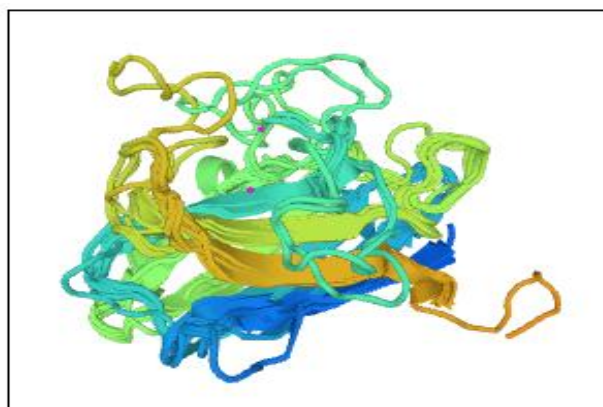
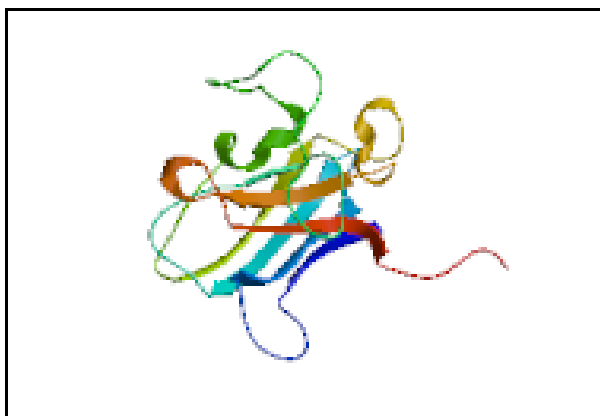
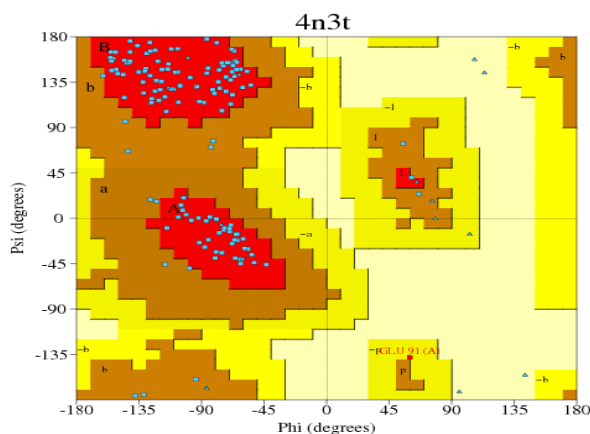


Fig.6: Target-Template Alignment showed overall 184 templates out of them the selected template Cu/Zn superoxide dismutases (4n3t.1.A) were used to build this model.



**Fig.7: Modeled protein image created by aligning the Target-template models.**

The stereo chemical high-quality of the 3D model was validated by using Ramachandran plot utilising RAMPAGE server. Fig.8 and Table 2 indicates that around 10.2% residues were present in the allowed regions, 89.1% residues in the favored region and most effective 0.8% residues were present in the outlier region indicating that the quality of the model was good.



**Fig. 8: Ramachandran plot of the PDB model from Fig.7 using RAMPAGE.**

**Table 2: Ramachandran Plot statistics for Zn-Cu SOD homology model using RAMPAGE server.**

Amino acid residues and regions (%)	Percentage
Residues in most favored regions [A,B,L]	89.1 %
Residues in the allowed [a,b,l,p]	10.2 %
Residues in the outlier regions	0.8 %

The quality of estimated model is based on the QMEAN scoring function were normalized with admire to the number of interactions<sup>[20]</sup>. The QMEAN score of the model was 0.62 and the Z-score was -2.02, which was very close to the value of 0 and this shows the fine quality of the model<sup>[21-22]</sup> because the estimated reliability of the model was expected to be in between 0 and 1 and this could be inferred from the density plot for QMEAN scores of the reference set (Fig.9A). A

comparison between normalized QMEAN score (0.40) and protein size in non-redundant set of PDB structures in the plot revealed different set of Z-values for different parameters such as C-beta interactions (-0.02), interactions between all atoms (-1.02), solvation (-0.84), torsion (-1.52) showed in (Fig. 9B).

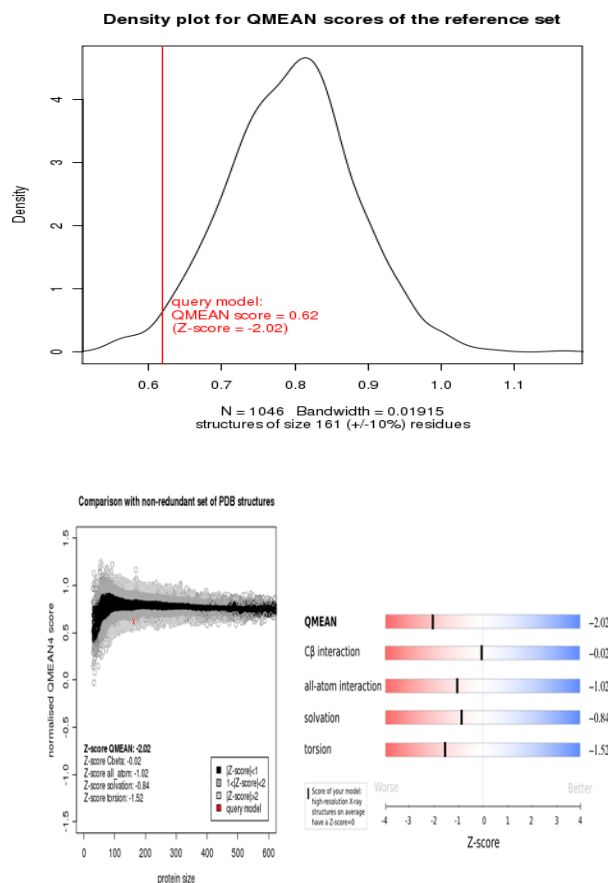


**Fig. 9: (A) The density plot for QMEAN showing the value of Z-score and QMEAN score (B) plot showing the QMEAN value as well as Z-score.**

Metalloproteins are proteins capable of binding one or more metal ions, which may be required for their biological function, for regulation of their activities or for structural purposes. Metal-binding properties remain difficult to predict as well as to investigate experimentally at the whole-proteome level. Consequently, the current knowledge about metalloproteins is only partial. In this paper the protein with 7 metal binding sites shows highest metal binding probability for the metal namely calcium in sites 2,3,4 & 7 with the metal probability of **0.691595**, **0.627722**, **0.398702** & **0.304824**; **Copper** in sites 1 & 5 with the probability of **0.407987** & **0.520100** and zinc in sites 1, 4, 6 & 7 with the probability of **0.473539**, **0.411537**, **0.595477** & **0.527491** showed in (Fig.10).

Table 3.

Protein	Metal Binding Sites	Metal binding probability								Metal Binding Pockets	
		CA	CO	CU	FE	MG	MN	NI	ZN	Amino acids	Position
P4	Site-1	0.0317	0.0217	<b>0.4080</b>	0.0332	0.0176	0.0119	0.0024	<b>0.4735</b>	H*	91
										H*	93
										G	107
										H*	109
										E*	117
										Q	130
										D*	133
										V	173
										H*	175
	R	181									
	Site-2	<b>0.6916</b>	0.0139	0.0167	0.0524	0.0590	0.0400	0.0080	0.1186	G	81
										P*	83
										E*	84
										F	88
										F	176
	Site-3	<b>0.6277</b>	0.01676	0.0201	0.0632	0.0712	0.0482	0.0096	0.1432	F*	176
										P*	177
										K*	179
										T*	180
	Site-4	<b>0.3987</b>	0.0139	0.0167	0.0523	0.0589	0.0399	0.0080	<b>0.4115</b>	K	61
										N*	76
										E*	78
										S	149
	Site-5	0.1277	0.0168	<b>0.5201</b>	0.0632	0.0712	0.0482	0.0096	0.1432	S*	151
										I	92
										D*	169
	Site-6	0.2518	0.0111	0.0134	0.0422	0.0475	0.0321	0.0064	<b>0.5955</b>	S*	171
										A	94
K										95	
F										110	
P										112	
T										113	
E										114	
Q										130	
V										160	
S										163	
D*										164	
A										165	
F										167	
L										168	
D*	169										
R	170										
Site-7	0.3048	0.0123	0.0147	0.0463	0.0521	0.0353	0.0071	<b>0.5275</b>	G	70	
									V	71	
									P	112	
									T	113	
									R	115	
									I	131	
									K	155	
									Y*	156	
									A	157	
									S	158	
									S	163	
D*	164										

**CONCLUSION**

Cell wall plays a key position in controlling shape and defending the fungi and other organisms from the atmosphere. It involves molecules which are integrated in morphogenesis, proliferation, cell-cell and cell-network associations. Zinc influences diverse mechanisms of fungal pathogenesis by directly associating with virulence determinants (i.e., metallo-proteases or SODs) or by regulating the expression of many proteins required for infection. This paper shows the different tools for homology modelling and structural CWBPs by using like SOPMA for secondary structure prediction, Phylogenetic tree was then constructed to determine the evolutionary relationships. Model validation was done by using Ramchandran plot and metal binding sites.

**ACKNOWLEDGMENT**

The authors are grateful to Prof. S. Rama Krishna Rao, Vice-Chancellor, KRU for providing the facilities required for the present work.

**CONFLICT OF INTEREST**

None of the authors have conflict of interest.

**REFERENCE**

1. Harold J. G. Meijer, Peter J. I. van de Vondervoort, Qing Yuan Yin, Chris G. de Koster, Frans M. Klis, Francine Govers, and Piet W. J. de Groot. "Identification of Cell Wall-Associated Proteins from *Phytophthora ramorum*", *Molecular Plant-Microbe Interactions*, 2006; 19(12): 1348-1358.
2. Sundstrom, P. 2002. Adhesion in *Candida* spp. *Cell Microbiol.* 4:461-469. Theodoropoulos, G., Hicks, S. J., Corfield, A. P., Miller, B. G., and Carrington, S. D. 2001. The role of mucins in host-parasite interactions: Part II—helminth parasites. *Trends Parasitol.* 17:130-135.
3. Marta Vallino, Elena Martino, Francesca Boella, Claude Murat, Marco Chiapello & Silvia Perotto, "Cu,Zn superoxide dismutase and zinc stress in the metal-tolerant ericoid mycorrhizal fungus *Oidiodendron maius* Zn", 2009 Federation of European Microbiological Societies, *Microbiol Lett* 293 (2009) 48–57
4. Charley C. Staats, Livia Kmetzsch, Augusto Schrank, and Marillene H. Vainstein, "Fungal zinc metabolism and its connections to virulence", *Front cell Infect Microbiol*, 2013; 3: 65.
5. Altschul, S.F., Madden, T.L., Schaffer, A.A., Zhang, J., Zhang, Z., Miller, W. and Lipman, D.J. (1997) Gapped BLAST and PSI-BLAST: a new generation of protein database search programs. *Nucleic Acids Res*, 25, 3389-3402.
6. Remmert, M., Biegert, A., Hauser, A. and Soding, J. HHblits: lightning-fast iterative protein sequence searching by HMM-HMM alignment. *Nat Methods*, 2011; 9: 173-175.
7. Guex, N. and Peitsch, M.C. SWISS-MODEL and the Swiss-PdbViewer: an environment for comparative protein modeling. *Electrophoresis*, 1997; 18: 2714-2723.
8. Sali, A. and Blundell, T.L. Comparative protein modelling by satisfaction of spatial restraints. *J Mol Biol*, 1993; 234: 779-815.
9. Dereeper A., Audic S., Claverie J.M., Blanc G. BLAST-EXPLORER helps you building datasets for phylogenetic analysis. *BMC Evol Biol.* Jan 12; 2010; 10: 8. (PubMed).
10. Chevenet F., Brun C., Banuls AL., Jacq B., Chisten R. TreeDyn: towards dynamic graphics and annotations for analyses of trees. *BMC Bioinformatics.* Oct 10, 2006; 7: 439. PubMed).
11. The UniProt Consortium, 2012. Reorganizing the protein space at the Universal Protein Resource (UniProt). *Nucleic Acids Res.*, 40: D71-D75.
12. Altschul, S.F., W. Gish, W. Miller, E.W. Myers and D.J. Lipman, Basic local alignment search tool. *J. Mol. Biol.*, 1990; 215: 403-410.
13. Lovell, S.C., I.W. Davis, W.B. Arendall III, P.I.W. de Bakker and J.M. Word et al., Structure validation by C $\alpha$  geometry:  $\eta$ ,  $\psi$  and C $\beta$  deviation. *Proteins: Struct., Funct., Genet.*, 2002; 50: 437-450.
14. Bowie, J.U., R. Luthy and D. Eisenberg, A method to identify protein sequences that fold into a known three-dimensional structure. *Science*, 1991; 253: 164-170.
15. Colovos, C. and T.O. Yeates, Verification of protein structures: Patterns of nonbonded atomic interactions. *Prot. Sci.*, 1993; 2: 1511-1519.
16. Benkert, P., Biasini, M. and Schwede, T. Toward the estimation of the absolute quality of individual protein structure models. *Bioinformatics*, 2011; 27: 343-350.
17. Mariani, V., Kiefer, F., Schmidt, T., Haas, J. and Schwede, T. Assessment of template based protein structure predictions in CASP9. *Proteins*, 2011; 79(Suppl 10): 37-58.
18. Combet C., Blanchet C., Geourjon C. and Deleage G. NPS@: Network Protein Sequence Analysis. *TIBS*, March 2000; 25(3)[291]: 147-150.
19. Rost, B., Twilight zone of protein sequence alignments. *Protein Eng.*, 1999; 12: 85-94.
20. Yang, A.S. and B. Honig, An integrated approach to the analysis and modeling of protein sequences and structures. III. A comparative study of sequence conservation in protein structural families using multiple structural alignments. *J. Mol. Biol.*, 2000; 301: 691-711.
21. Wiederstein, M. and M.J. Sippl., ProSA-web: interactive web service for the recognition of errors in three-dimensional structures of proteins. *Nucleic Acids Research*, 2007; 35: 407-410.
22. Prajapat, R., A. Marwal and R.K. Gaur, 2014. Recognition of Errors in the Refinement and validation of three-dimensional structures of AC1 proteins of begomovirus strains by using ProSA-Web, *Journal of Viruses.*, 2014: doi.org/10.1155/2014/752656.